Am J Transl Res 2017;9(3):1025-1036
www.ajtr.org /ISSN:1943-8141/AJTR0044376

Original Article

Geniposide inhibited endothelial-mesenchymal transition via the mTOR signaling pathway in a bleomycin-induced scleroderma mouse model

Qing Qi[1,2*], Yueping Mao[3*], Yongzhen Tian[1], Ke Zhu[1], Xushan Cha[1], Minghua Wu[2], Xiaodong Zhou[2]

[1]Department of Dermatology, The First Affiliated Hospital, Guangzhou University of Chinese Medicine, Guangzhou 510405, China; [2]Division of Rheumatology and Clinical Immunogenetics, Department of Internal Medicine, University of Texas Health Science Center at Houston, Houston 77030, Texas, USA; [3]Department of Dermatology, Sun Yat-Sen Memorial Hospital, Sun Yat-Sen University, Guangzhou 510120, China. [*]Equal contributors and co-first authors.

Received November 15, 2016; Accepted February 26, 2017; Epub March 15, 2017; Published March 30, 2017

Abstract: Aim: Geniposide is an iridoid glycoside isolated from the gardenia plant. It has multiple biological activities. The roles of geniposide in systemic sclerosis (SSc) and in endothelial-to-mesenchymal transition (EndMT) are unclear. We investigated the protective effects of geniposide in a bleomycin-induced SSc mouse model, and its potential mechanisms. Methods: The effects of geniposide were evaluated as follows: (1) histological and immunochemical changes in mouse skin tissue; (2) changes in cellular morphology of human umbilical vein endothelial cells (HUVECs); (3) expression of endothelial cell biomarkers (E-Cadherin, CD31, and CD34), mesenchymal cell markers (FSP1, Collagen, and α-SMA), and key factors of EndMT (Slug, Snail, and Twist) using real time PCR, Western blot, and immunofluorescence; (4) tube formation in HUVECs; (5) mTOR signaling pathway transcription factors using Western blot analysis. Results: Treatment with bleomycin induced up-regulation of mesenchymal cell biomarkers and down-regulation of endothelial cell biomarkers in *in vivo* and *in vitro* bleomycin-induced scleroderma models. Geniposide treatment suppressed these effects. Geniposide remedied bleomycin-induced dermal capillary loss and fibrosis in mice. The expression of key EndMT factors (Slug, Snail, and Twist) and the mTOR signaling pathway (mTOR and S6) were also attenuated by geniposide treatment. Conclusion: Geniposide had protective effects on endothelial cells in the bleomycin-induced scleroderma mouse model. These effects may occur via inhibition of the mTOR signaling pathway activation. The results suggested that geniposide could be a potential candidate drug for treatment of vascular damage in SSc patients.

Keywords: Geniposide, bleomycin, endothelial-to-mesenchymal transition, systemic sclerosis

Introduction

Systemic sclerosis (SSc) or scleroderma is a chronic disease characterized by immune system activation, vasculopathy, and tissue fibrosis [1]. The vascular abnormalities that cause organ dysfunction, particularly in the lung, heart, and kidney [2] likely drive the Raynaud's phenomenon that is the first symptom of the disease. Different mediators (e.g., endothelin-1 (ET-1) and transforming growth factor-β (TGF-β)) have been identified as involved in the vascular remodeling that occurs in SSc patients [3]. However, the underlying mechanisms of SSc vasculopathy and how damage results in fibrosis are poorly understood. Studies have revealed that perivascular myofibroblasts may originate from the mesenchymal transition of endothelial cells (ECs). This endothelial-to-mesenchymal transition (EndMT) is a possible pathogenic mechanism for diseases including diabetic nephropathy, cardiac fibrosis, intestinal fibrosis, pulmonary hypertension, and SSc [4-9].

Bleomycin (BLM)-induced fibrosis mouse models are widely used to investigate pulmonary fibrosis [10]. The SSc mouse model was first used by Yamamoto; it was developed to reproduce dermal and lung fibrosis with pro-fibrotic inflammation, vascular wall thickness in the

deep dermis, and serum autoantibody production [10-12]. BLM can induce production of reactive oxygen species, which damage the surrounding cells and result in adverse consequences such as up-regulation of adhesion molecules, leukocyte infiltration, and resident fibroblast activation [13]. Taken together, these responses suggest that BLM can induce early inflammation and late stages of fibrosis, similar to the responses that occur during SSc pathogenesis [13].

The BLM-induced model has been used to examine the EndMT [14-16]. The EndMT was first revealed in 1975 by developmental studies of heart formation [17]. It is characterized by loss of cell-cell adhesion and changes in cell polarity, which induce a spindle-shaped morphology. These changes are accompanied by reduced expression of endothelial markers (e.g., vascular endothelial cadherin and CD31), and increased mesenchymal marker expression (e.g., fibroblast-specific protein-1, α-smooth muscle actin (α-SMA), neural cadherin, and fibronectin) [18]. Loss of cell-cell adhesion is mediated by transcription factors such as Snail, Slug, zinc finger E-box-binding homeobox 1, SIP-1, Twist, and lymphoid enhancer-binding factor-1, which suppress the transcription of genes encoding proteins involved in the formation of both adherent junctions and tight junctions [19-22].

Mammalian target of rapamycin (mTOR) has broad anti-proliferative properties. mTOR signaling affects major cellular functions; it has a significant role in regulation of basic cell behaviors such as growth (mass accumulation) and proliferation. mTOR deregulation occurs in many human diseases, such as cancer, obesity, type 2 diabetes, and neurodegeneration [23]. Significant pharmacological studies are targeting this pathway. The BLM-induced transformation may be regulated by the EndMT-related transcription factor Slug in an Akt/mTOR pathway-dependent manner [24].

Traditional herbal medicine has long been used to relieve SSc symptoms in patients in China, but the therapeutic mechanisms of action are unclear. Our previous study revealed that one substance from an herbal compound (Astragaloside IV) claiming to “nourish the kidney and strengthen the essence” exhibited anti-fibrotic effects via the TGF-β/SMAD3 pathway [25]. However, because any given Chinese herbal compound usually consists of hundreds of constituents, studies of therapeutic efficacy should include a comprehensive analysis of each component. In this study, we isolated one of these important substances, geniposide, which is derived from the Chinese herbal compound Zhizi. Results using the BLM-induced SSc model indicated that geniposide protects ECs. The Chinese Pharmacopoeia describes the herbal medicine Zhizi as the dried fruit of *Gardenia jasminoides* and that it has “bitterness and coldness” properties. According to traditional Chinese medicine theory, a herbal medicine with these properties could be considered for application in various inflammatory conditions, including the early inflammation experienced by SSc patients. The pharmacological activities of geniposide (an iridoid glycoside) include anti-oxidation, anti-tumor, anti-asthma, and anti-diabetic effects [26-29]. An increasing number of studies have examined the therapeutic role of geniposide in brain diseases, especially ischemic cerebral vascular disease. Geniposide has a protective effect on the granule cell layer and can reduce neuronal cell death induced by oxygen and glucose deprivation [30]. Yin *et al*. examined the cytoprotective effects of geniposide on hippocampal neurons and found that it induces nuclear translocation of nuclear factor-E2-related factor 2 (Nrf2) [31]. Park *et al.* found that geniposide suppresses liver fibrosis by targeting the TGF-β/SMAD3 and ERK-MAPK pathways. This mechanism of action may also be relevant for treatment of fibrotic diseases (e.g., SSc) [32].

No studies have used a BLM-induced SSc mouse model to examine the effects or underlying mechanisms of geniposide treatment. The objective of this study was to use a BLM-induced SSc model to evaluate geniposide efficacy and effects on the EndMT and on the mTOR signaling pathway.

Materials and methods

Ethics statement

The study protocol was approved by the animal ethics committee of the Guangzhou University of Chinese Medicine. The ethics committee of the First Affiliated Hospital, Guang Zhou University of Chinese Medicine, approved the collection of tissue samples for the study.

Table 1. Primers used in the RT-PCR assay

Primers	Sequences (5'→3')
H-E-cadherin-F	GAGAAACAGGATGGCTGAAGG
H-E-cadherin-R	TGAGGATGGTGTAAGCGATGG
H-Snail-F	ACCACTATGCCGCGCTCTT
H-Snail-R	GGTCGTAGGGCTGCTGGAA
H-CD31-F	AGGCATTTTGGACCAAGCAG
H-CD31-R	GGCCGCAATGATCAAGAGAG
H-collagen I F	GCCAAGACGAAGACATCCCA
H-collagen I R	GGCAGTTCTTGGTCTCGTCA
H-α-SMA F	TGCCTTGGTGTGTGACAATG
H-α-SMA R	TCACCCACGTAGCTGTCTTT
H-CD34-F	TAGCCTTGCAACATCTCCCA
H-CD34-R	CTTAAACTCCGCACAGCTGG
H-Slug-F	CAACGCCTCCAAAAAGCCAA
H-Slug-R	ACTCACTCGCCCCAAAGATG
Mus-Slug-F	GAACCCACACATTGCCTTGT
Mus-Slug-R	GCAGAAGCGACATTCTGGAG
H-twist-F	AGTCTTACGAGGAGCTGCAG
H-twist-R	AGGAAGTCGATGTACCTGGC
Mus-twist-F	CAGCGGGTCATGGCTAACG
Mus-twist-R	TTGCTCAGCTTGTCCGAGG
H-FSP1-F	TTGTCCCTGTTGCTGTCCAA
H-FSP1-R	TTGTCCCTGTTGCTGTCCAA
Mus-snail-F	AAGCCCAACTATAGCGAGCT
Mus-snail-R	TTTTGCCACTGTCCTCATCG
β-actin-F	CCCATCTATGAGGGTTACGC
β-actin-R	TTTAATGTCACGCACGATTTC

Animals, cells, and treatment

C57Bl/6J female mice (body weight range, 20-22 g) were obtained from the laboratory animal center of Sun Yat-Sen University (Guangzhou, China). BLM (Nippon Kayaku, Tokyo, Japan) was dissolved in PBS at a concentration of 1 mg/ml and sterilized by filtration, BLM was injected subcutaneously into the shaved backs of the mice daily for 4 weeks with a 27-gauge needle. The SSc mouse model was established. Each SSc mouse was randomly allocated to one of four groups (Control, BLM, BLM+geniposide (BLM+GEN), or BLM+rapamycin (BLM+Rap)). Each mouse received a daily subcutaneous injection in the same site in the back skin for 4 weeks. Each Control group mouse was injected with 100 ul phosphate buffered saline (PBS) per day. Each BLM mouse was injected with 100 ul BLM in PBS (1 mg/ml) per day. The BLM+GEN mice were each injected with 100 ul/day BLM (1 mg/ml) and geniposide (40 mg/kg/day). The BLM+Rap mice were injected with 100 ul/day BLM (1 mg/ml) and rapamycin (1.5 mg/kg/day). At the end of the 4-week period, each mouse was euthanized and the skin tissue was harvested and processed for analysis.

The human umbilical vein endothelial cell (HUVEC) line was obtained from the American Type Culture Collection (ATCC, Manassas, VA, USA) and cultured in Roswell Park Memorial Institute 1640 medium containing 10% fetal bovine serum. The HUVEC cells were divided into four treatment groups. The control group cells were treated with PBS; the BLM group cells were treated with BLM (0.1 mU/mL); the BLM+GEN cells were treated with BLM (0.1 mU/mL) and geniposide (200 μg/ml); the BLM+Rap cells were treated with BLM (0.1 mU/mL) and rapamycin (100 nM). After 48 hours of stimulation, the cells were harvested and analyzed for mRNA and protein expression.

Real-time quantitative PCR (RT-PCR)

The HUVEC cells and skin tissues were homogenized and total RNA was extracted using the RNeasy MiniKit (Qiagen, Germany). RNA quantity was normalized to 18s rRNA. One microgram total RNA was used for random hexamer reverse-transcription. The cDNAs were amplified using the GoTaq® qPCR Master Mix (Promega, Madison, USA) following the manufacturer's instructions and a MiniOpticon™ real-time PCR detection instrument (Bio-Rad, CA, USA). β-actin was used as an internal control. The primers used for the amplification are presented in **Table 1**. The results were normalized to the control group and relative fold changes were determined using the ($2^{-\Delta\Delta Ct}$) method. The Ct values provided from real-time quantitative PCR instrumentation were imported into Microsoft excel, and the change in expression of the target gene was normalized to β-actin.

Western blot analysis

Homogenization in a RIPA buffer (Beyotime Biotechnology, Shanghai, China) was used to prepare the HUVEC lysates. The protein concentrations were determined using a Bicinchoninic Acid Protein Assay Kit (Pierce, Rockford, IL, USA). The lysates were denatured at 95°C for 5 min; 50 mg total protein per lane was used for the SDS-polyacrylamide gel electrophore-

sis. The proteins were blotted on polyvinylidene difluoride membranes (Thermo Fisher Scientific, MA, USA), followed by blocking with 5% skimmed milk for 1 h at room temperature. The proteins were blotted using anti-E-cadherin antibody (1:1,000; Cell Signaling Technology, Inc., MA, USA), anti-CD31 antibody (1:1,000; Cell Signaling Technology, Inc.), anti-FSP1 antibody (1:200; Sigma Aldrich, MO, USA), anti-α-SMA antibody (1:1,000; Assay Biotechnology, Co., Inc., CA, USA), anti-Slug antibody (Cell Signaling Technology, Inc.), anti-Snail antibody (1:1,000; BD Biosciences, Franklin, NJ, USA), anti-Twist antibody (1:500; Abcam, MA, USA), anti-p-S6 antibody (1:1,000; Cell Signaling Technology, Inc.), anti-S6 antibody (1:1,000; Cell Signaling Technology, Inc.), anti-p-mTOR antibody (1:1,000; Cell Signaling Technology, Inc.), or anti-mTOR antibody (1:1,000; Cell Signaling Technology, Inc.). An anti-GAPDH (Sigma Aldrich) antibody was used as the internal control. The blots were visualized using chemiluminescence (Forevergen, Guangzhou, China). All experiments were performed in triplicate. Selected blots were quantified using Image J software.

Image analysis

The morphology of cells without pigmentation was examined under the optical microscope (Eclipse TS100, Nikon Instruments Inc., NY, USA).

Immunohistochemistry

Five microns of the paraffin-embedded tissue from each skin sample were deparaffinized using Histo-Clear (National Diagnostics, Atlanta, GA), rehydrated, and washed with 0.01 M PBS. The endogenous peroxidase activity was blocked using 3% hydrogen peroxide in methanol at room temperature for 30 min. After blocking in 10% goat serum for 30 min, each section was incubated with α-SMA (1: 100, Santa Cruz, CA, USA) and Snail antibodies (1:50, Abcam, MA, USA) at 4°C overnight, followed by HRP-conjugated secondary antibody exposure at 37°C for 1 h. The ABC (Vector, Laboratories, CA, USA) and DAB substrate (Sigma, Schnelldorf, Germany) kits were used according to the manufacturer's protocol to visualize the results. The stained samples were counted in 10 random grids under high magnification power fields of a light microscope. Each section was examined independently by two investigators in a blinded manner.

Immunofluorescence

Paraffin-embedded tissue from each skin sample was deparaffinized and rehydrated. Antigen retrieval was performed in citrate buffer. Endogenous peroxidase activity was blocked by incubating slides for 30 minutes in 0.3% H_2O_2; the slides were then incubated in 0.1 M glycine for 45 minutes at 48°C. Blocking was performed in 3% rabbit serum or 3% goat serum (vWF) for 1 hour, followed by overnight incubation with E-cadherin (1:50, Cell Signaling Technology), CD31 (1:50, Cell Signaling Technology), α-SMA (1:200, Assay Biotechnology), or Snail (1:100, BD Biosciences). Each slide was then incubated in the FITC-conjunct secondary antibody (Invitrogen, CA, USA) for 30 minutes. The cell nuclei were stained using Hoechst 33258 stain (Invitrogen) and the images were captured using fluorescence microscopy (Olympus BX51W1, Tokyo, Japan).

Hematoxylin and eosin and cs

The samples stained with hematoxylin and eosin (HE) were prepared as following. Each sample was fixed in 10% buffered formalin, embedded in paraffin and routinely processed. Three to five micrometer thick sections were stained with hematoxylin (Sigma H 3136) for 10 min and with eosin (Sigma E 4382) for 1 min to visualize the areas for examination. The samples stained using the Fontana-Masson method, Fontana-Masson staining of the samples was performed following the protocol provided in the Fontana-Masson kit (Abcam, ab150669).

Matrigel tube formation assay

HUVEC cells were seeded at a density of 1×10^4 cells/well in basement membrane matrix gel (Matrigel, BD) coated on two-well glass slides and pretreated with PBS, BLM, BLM+GEN, or BLM+Rap. After 48 hours of treatment, the cell culture medium was replaced with serum-free medium and was incubated for 8 hours at 37°C in a humidified incubator (5% CO_2). Six fields from each group were randomly selected for inverted microscopy examination for quantification of tube formation. The tube lengths were calculated and the results were normalized to the control group values.

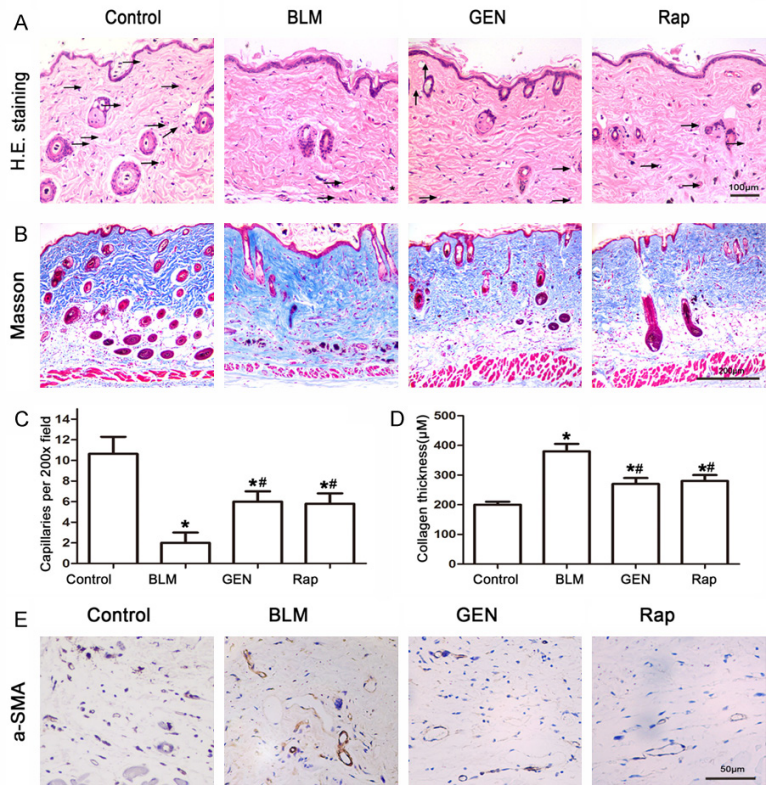

Figure 1. Image analysis of BLM- and geniposide-treated murine skin tissues. C57BL/6 mice received PBS, BLM, BLM and geniposide, or BLM and rapamycin treatments for 4 weeks; skin tissues were then harvested for analysis. A. H&E stain results for mouse skin tissue for the four treatments. Representative images. Black arrows indicate blood vessels. B. Fontana-Masson stain results for the four treatment groups. Representative images. C. Computerized histogram analysis of capillaries, *P<0.05, compared with control group; #P<0.05, compared with BLM group. D. A histogram of the values for collagen thickness, *P<0.05, compared with control group; #P<0.05, compared with BLM group. E. Immunohistochemistry analysis of the mesenchymal marker α-SMA, scale= 50 μm.

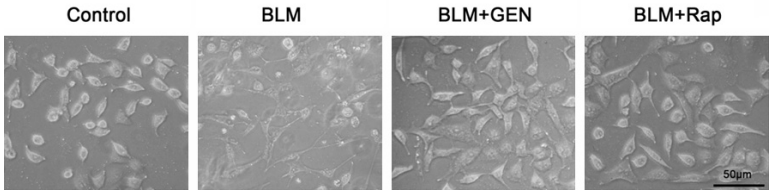

Figure 2. Cell morphology changes after bleomycin and geniposide treatment of HUVECs *in vitro*. Confluent HUVECs were stimulated with PBS, BLM, BLM and geniposide, or BLM and rapamycin under identical conditions. After 48 hours of stimulation, cell morphology was observed under the microscope. Representative images. Scale=50 μm.

Statistical analysis

SPSS software, version 18.0 (IBM, NY, USA) was used for the statistical analysis. The results were presented as mean ± standard deviation values. The Student's t-test was used to analyze differences between two groups. One-way analysis of variance was used to analyze differences between more than three groups. A *P*-value <0.05 was considered to indicate a statistically significant result.

Results

Geniposide successfully inhibited BLM-induced dermal capillary loss and fibrosis in mice

We first used our BLM-induced animal model to investigate the effects of geniposide. We treated C57BL/6J wildtype mice with BLM or BLM plus geniposide for 4 weeks. Rapamycin was used as a positive control for mTOR inhibition because a previous study found that it is involved in BLM-induced EndMT in HUVECs (24). The H&E stain results indicated that compared with the Control group mice, the skin samples from the BLM group mice had thick and compact collagen fibers and a reduction in the number of blood vessels; the Control mice had skin with a low density of collagen fibers and high density of blood vessels (**Figure 1**). Collagen fiber deposition was reduced in the BLM group, and blood vessel number was increased in the GEN and Rap treatment groups (**Figure 1A**). The Fontana-Masson staining revealed that the severe cutaneous fibrosis induced by BLM treatment of the BLM group mice was effectively attenuated in the GEN and Rap treatment groups (**Figure 1B**). The immunohistochemistry analysis revealed that the number of cells positive for α-SMA was reduced in the GEN group and the Rap group, compared with the BLM group mice (**Figure 1E**). These results indicated that geniposide

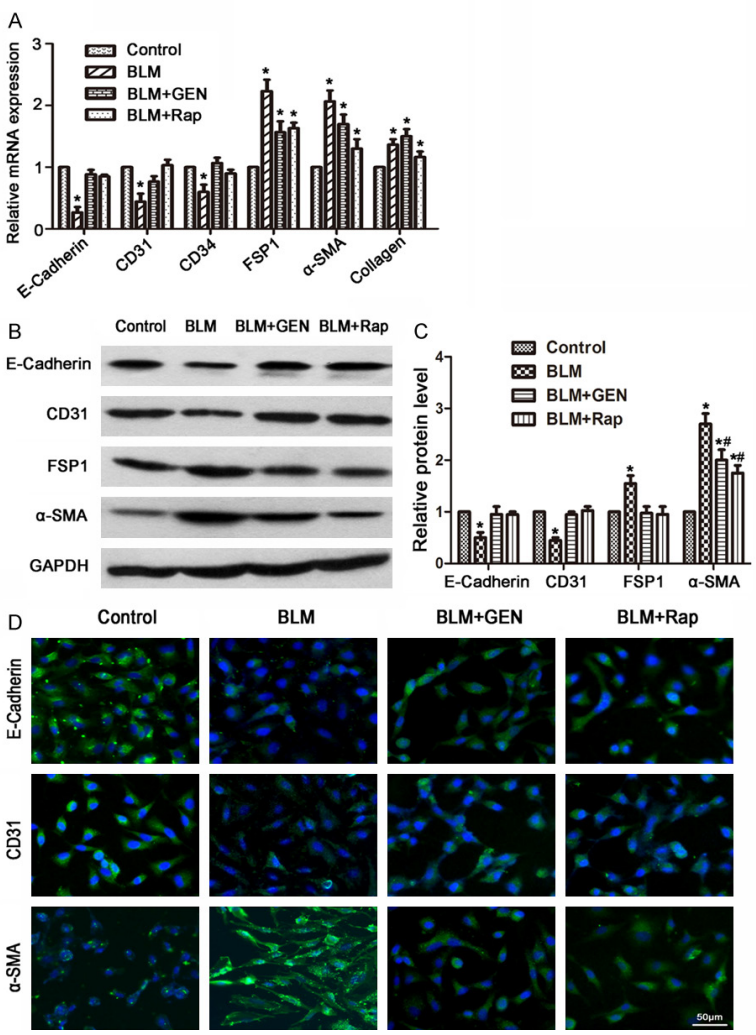

Figure 3. Effects of geniposide on the expression of endothelial and mesenchymal cell biomarkers in HUVECs treated with BLM and geniposide. HUVECs were treated with PBS, BLM, BLM and geniposide, or BLM and rapamycin for 48 hours and harvested for analysis. A. mRNA expression using RT-PCR analysis. Relative expression was quantified using the ΔΔCt method and represented as fold change, normalized to control group values. *P<0.05, compared with control group. B. Western blot results. C. A histogram depicting the relative protein level in each group, *P<0.05, compared with control group; #P<0.05, compared with BLM group. D. Immunofluorescence analysis was performed to detect the expression levels of E-Cadherin, CD31, and α-SMA.

had an important role in fibrosis and EndMT inhibition in this BLM-induced SSc mouse model.

Geniposide inhibited EndMT in HUVECs in vitro

We evaluated the EndMT and the cell morphological changes caused by BLM or BLM plus geniposide treatments in HUVECs *in vitro*. HUVEC cells in the PBS (Control) treatment group did not induce changes in EndMT-associated cell shape. The BLM group cells had a spindle-shaped fibroblast-like morphology after 48 hours of BLM treatment. Geniposide treatment inhibited the fibroblast-like morphology changes caused by BLM treatment (**Figure 2**). The real-time PCR results indicated that compared with the control group cells, the expression of EC biomarkers (E-Cadherin, CD31, and CD34) in the BLM group was significantly down-regulated and the mesenchymal cell biomarkers (FSP1 and α-SMA) and collagen I α2 mRNA were significantly up-regulated (**Figure 3A**). There were no statistically significance differences in expression of EC biomarkers (E-Cadherin, CD31, and CD34) in the BLM+Rap group or in the BLM+GEN group, compared with the control group cells (**Figure 3A**).

Western blot analysis revealed that BLM challenge decreased expression of biomarkers in ECs (E-Cadherin and CD31), which can be resisted using treatment with geniposide and rapamycin (**Figure 3B**, **3C**). BLM treatment resulted in overexpression of FSP1 and α-SMA proteins in HUVECs, compared with the control group cells. These effects were also inhibited by geniposide or rapamycin treatment. Immunofluorescence analysis revealed that compared with the control group cells, E-Cadherin and CD31 were significantly down-regulated and α-SMA was up-regulated in the BLM group cells; these changes were inverted by using geniposide or rapamycin treatment (**Figure 3D**).

We also performed experiments to examine the effect of geniposide on tube formation. After 8 hours of incubation with BLM or geniposide, cell formation was randomly photographed us-

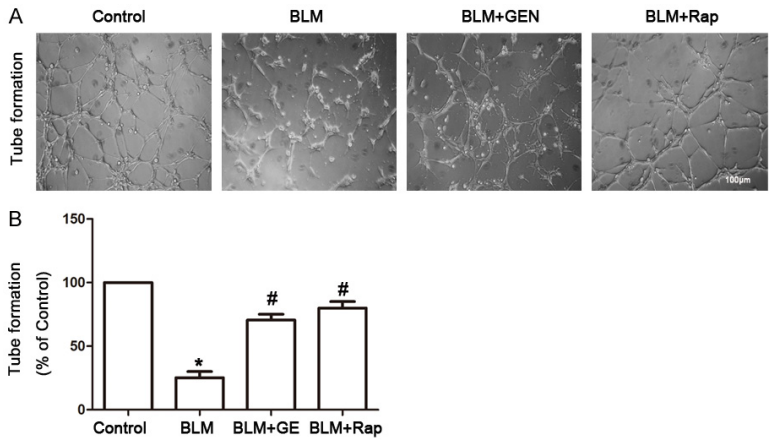

Figure 4. Geniposide restored tube formation in HUVECs *in vitro*. HUVECs were seeded in a basement membrane matrix gel and treated with PBS, BLM, BLM and geniposide, or BLM and rapamycin. After 8 h of incubation, six fields from each cell group were randomly photographed using inverted microscopy; tube lengths were calculated using an image analysis system. A. Representative images. B. Tube formation analysis (Image J software). N=6, *P<0.05, compared with control group; #P<0.05, compared with BLM group.

ing inverted microscopy and the results were analyzed. Geniposide and rapamycin treatment significantly restored tube formation, compared with the response in the BLM treatment group (**Figure 4A**, **4B**). Taken together, these results suggested that geniposide inhibited the BLM-induced EndMT by inducing tube formation, up-regulation of E-cadherin and CD31, and by inhibiting expression of SMA and FSP1. These results further indicated that geniposide had a potential role for inhibition of the BLM-mediated EndMT *in vitro*.

Geniposide inhibited the Slug and Snail EndMT transcriptional factors, in HUVECs in vitro

We performed *in vitro* experiments to evaluate the key EndMT factors in four treatment groups using real-time PCR [33]. The results indicated that the BLM+GEN and BLM+Rap groups had reduced expression of Slug, Snail, and Twist, compared with the BLM group (**Figure 5A**). Twist promoted up-regulation in the BLM group; upregulation was not statistically significant in the control group. Western blot analysis revealed that BLM treatment induced significantly increased protein expression of the key EndMT factors (Slug, Snail, and Twist); this effect was resisted by treatment with geniposide or rapamycin (**Figure 5B**, **5C**). Immunofluorescence analysis revealed that Snail expression was significantly up-regulated in the BLM treatment group compared with the control group, which was also inverted by treatment with geniposide or rapamycin (**Figure 5C**). In summary, geniposide effectively inhibited the expression of key factors during BLM-mediated EndMT in HUVECs *in vitro*.

Geniposide inhibited the mTOR signaling pathway in HUVECs in vitro

BLM can activate the Akt/mTOR signaling pathway and up-regulate phosphorylation levels of S6 (an mTOR signaling pathway protein) [23, 24]. We investigated the effects of geniposide on the mTOR signaling pathway. Western blot analysis revealed that BLM challenge did not affect total mTOR and S6 expression in HUVECs. However, BLM induced a significant up-regulation of phospho-mTOR and phospho-S6 expression by 48 hours post-treatment (**Figure 6A**, **6B**). The up-regulation of these phosphorylated proteins was suppressed by geniposide and rapamycin treatment. This result suggested that the BLM-induced up-regulated key factors in the mTOR signaling pathway can be inverted by treatment with geniposide. Taken together, these results suggested that the mTOR signaling pathway is involved in the regulation of geniposide's reversion of BLM-mediated EndMT.

Geniposide inhibited key EndMT factors in the BLM-induced mouse model in vivo

Transcriptional repressors of E-cadherin (e.g., Slug (SNAI2), Snail (SNAI1), and Twist) have been implicated in the EndMT in various embryonic development and tumor progression systems [34, 35]. To further understand the EndMT in an SSc animal model, we evaluated Slug, Snail, and Twist mRNA and protein levels in four treatments groups *in vivo*. The mRNA and protein levels of Slug and Snail were significantly up-regulated in the BLM treatment group, compared with the control group (**Figure 7A-C**). The results for the mRNA and protein levels indicated that treatment with geniposide or rapamycin for 48 hours significantly abrogated BLM-induced Slug and Snail expression. The

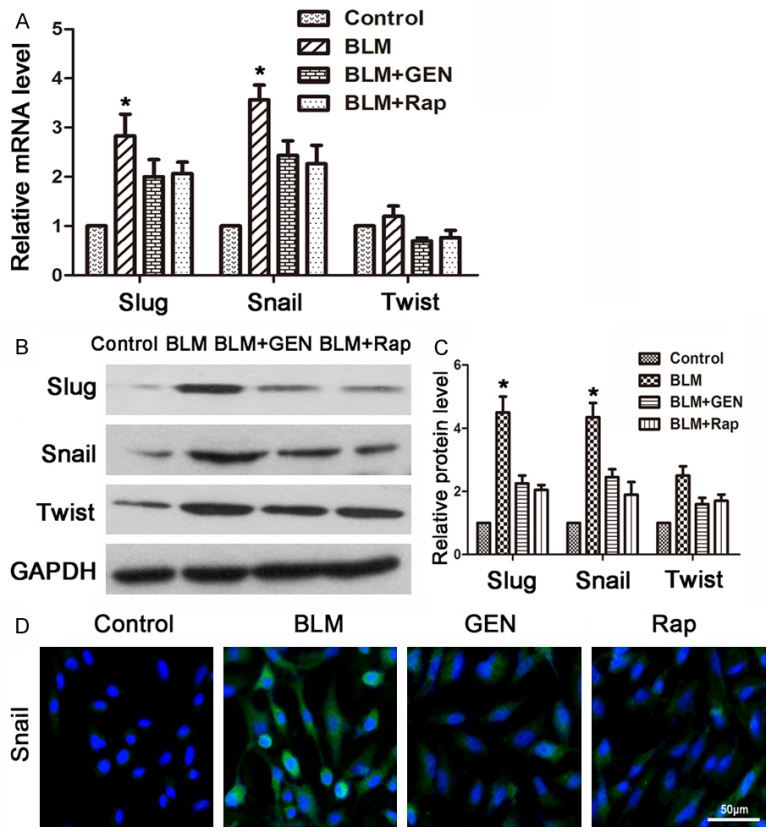

Figure 5. Expression of key factors during EndMT, bleomycin and geniposide treatments of HUVECs *in vitro.* HUVECs were treated with PBS, BLM, BLM and geniposide, or BLM and rapamycin for 48 hours and harvested for analysis. Control: treated with PBS; BLM: treated with bleomycin; BLM+GEN: treated with bleomycin and geniposide; BLM+Rap: treated with bleomycin and rapamycin (positive control). A. RT-PCR analysis. Relative expression was quantified using the ΔΔCt method, normalized to control values. The results are presented as fold change, *P<0.05, compared with control group values. B. Western blot analysis results. C. Histogram depicting the relative protein level in each group. D. Immunofluorescence results.

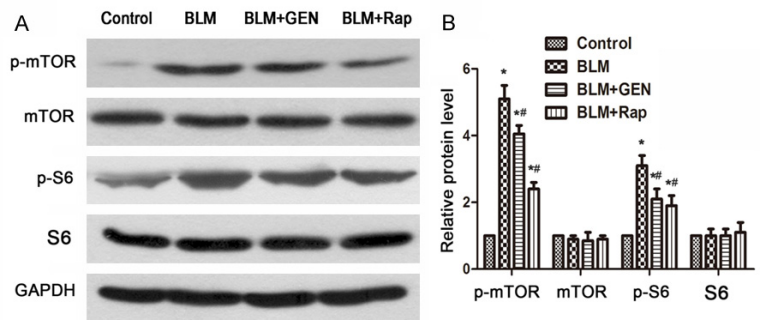

Figure 6. A. Expression of p-mTOR and mTOR, p-S6, and S6 stimulated with BLM and geniposide in HUVECs. Representative images. N=3. B. Relative protein level in each group (Image J software). N=3, *P<0.05, compared with control group; #P<0.05, compared with BLM group.

difference between the BLM+GEN and BLM+Rap groups was not statistically significant.

These results suggested that BLM treatment promoted increased expression of key factors (Slug, Snail, and Twist) of the EndMT, which can be inhibited by using geniposide treatment. Immunohistochemistry analysis revealed an increased number of Snail-positive ECs in the BLM treatment group compared with the control group. However, the numbers of Snail-positive ECs were significantly reduced in the BLM+GEN and BLM+Rap treatment groups (**Figure 7D**). Consistent with the results of our *in vitro* study, theseresultsindicatedthatgeniposide may have an important role in the inhibition of the EndMT in the SSc animal model.

Discussion

To our knowledge, this study is the first to examine the use of geniposide for SSc treatment and to explore its therapeutic effects on ECs. We found that geniposide protected ECs by inhibiting the BLM-induced EndMT *in vivo* and *in vitro*.

Accumulating evidence indicates that EndMT occurs during SSc. Angiotensin II has been implicated in the EndMT, which plays a role in the progression of fibrotic disease [36]. Stawski and colleagues found that Angiotensin II activates the TGF-β pathway, which promotes the EndMT and the ensuing inflammation by increasing myofibroblast accumulation. This process results in excessive collagen synthesis and deposition in mouse skin [37]. Mendoza *et al.* found that cells expressed endothelial and mesenchymal cell-specific markers in patients with interstitial lung dis-

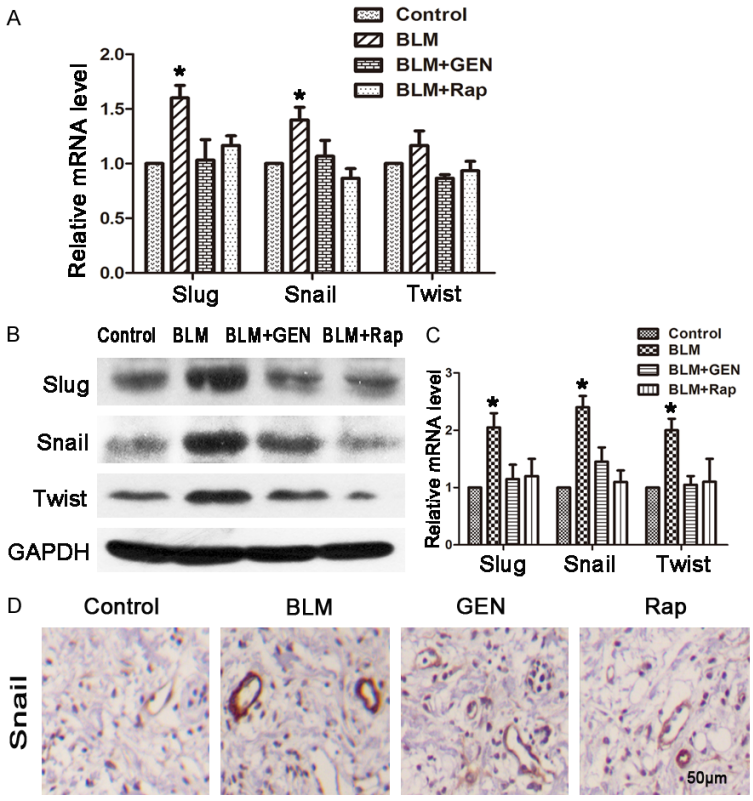

Figure 7. Key factors of the EndMT (Slug, Snail, and Twist) treated with bleomycin and geniposide in HUVECs. HUVECs were treated with combinations of BLM, geniposide, and rapamycin for 48 hours and harvested for analysis. Control: treated with PBS; BLM: treated with bleomycin; BLM+GEN: treated with bleomycin and geniposide; BLM+Rap: treated with bleomycin and rapamycin (positive control). A. RT-PCR; relative expression of mRNA was quantified using the ΔΔCt method, and presented as the fold change normalized to the control group value. *P<0.05, compared with control group. B. Western blot analysis results. C. Relative protein level in each group (Image J software). N=3, *P<0.05, compared with control group. D. Immunohistochemistry analysis results Scale= 50 μm.

ease (ILD) and that the EndMT occured in SSc-ILD patients [38]. Taken together, these results suggest that the EndMT has a role in SSc pathogenesis. Investigation of geniposide and the EndMT may result in development of new treatment strategies for SSc.

The EndMT may connect persistent endothelial injury and aberrant fibrogenesis, which are two hallmarks of SSc pathogenesis [39]. EC injury occurs in the very early stages of the disease, and the activated ECs undergo EndMT to become myofibroblasts in the blood vessel walls. This response contributes to the fibroproliferative vasculopathy. The myofibroblasts can migrate to surrounding areas of the vessel and participate in tissue fibrogenesis [40]. Our BLM-induced mouse model consistently revealed that geniposide reduced endothelial loss and dermal fibrosis via inhibition of the EndMT (**Figure 1**).

We used BLM to establish *in vivo* and *in vitro* EndMT models. Several studies have revealed the EndMT in BLM-induced lung and skin fibrosis animal models [14-16]. Zhang *et al.* found that BLM-induced ECs undergo the EndMT, processed in a Slug-dependent manner *in vitro* [24]. Our study revealed that BLM treatment resulted in the marked elimination of E-Cadherin and increased expression of the mesenchymal markers FSP1 and α-SMA. This result indicated that EndMT occurred in the HUVEC cells. The expression level of collagen I α2 was slightly higher in the BLM-stimulated cells than in the control cells. More significantly, the BLM+GEN treatment cells exhibited a significant up-regulation of EC biomarkers (E-Cadherin, CD31, and CD34) and down-regulation of mesenchymal cells (FSP1, collagen, and α-SMA), compared with the BLM-stimulated cells that did not undergo geniposide treatment. This result suggested that BLM-induced EndMT can be inverted by using geniposide treatment.

To further explore potential mechanisms, we examined mediators of the EndMT and mTOR pathways. EndMT and EMT are regulated by the basic helix-loop-helix transcription factors (e.g., Twist) and the zinc finger transcription factors (e.g., Snail and Slug) [3]. SNAIL1 (also known as Snail) and SNAIL2 (also known as Slug) can activate the EndMT during development, fibrosis, and cancer [41]. Our study results indicated that BLM increased *in vivo* and *in vitro* expression levels of the key EndMT factors (Slug, Snail, Twist), compared with the control groups (**Figures 5** and **7**). The up-regulation of Slug, Snail, and Twist in the BLM-

treated HUVECs (**Figure 5**) that occurred in this study suggested that BLM successfully induced the EndMT in the HUVECs, and that this effect was abrogated by geniposide treatment.

The complete mechanism of EndMT is largely unknown, but study results have suggested that several signaling pathways may be involved in regulation of the EndMT process. Cooley *et al.* found that endothelial-derived cells contribute to neointimal formation via EndMT, which involves activation of the Smad2/3-Slug signaling pathway [42]. Activation of the mTOR signaling pathway regulates BLM-induced EndMT [24]. Consistent with Zhang *et al*.'s findings, our results indicated that BLM induced significant up-regulation and activation of key factors in the mTOR signaling pathway, including p-mTOR and p-S6. Treatment with geniposide inverted this BLM-induced up-regulation of p-mTOR and p-S6. Taken together, our results suggested that geniposide may have a crucial role in blocking BLM-mediated EndMT in HUVECs, via the mTOR signaling pathway.

The mechanism for attenuation of fibrosis by geniposide in the BLM-induced animal model may include additional pathways. For example, geniposide may also suppress collagen I α2 via the inhibition of the TGF-β/SMAD3 and ERK-MAPK pathways during liver fibrosis [32]. There is no perfect model, and no one model can represent all the pathophysiologic characteristics of SSc. Therefore, observations based only on a BLM-induced SSc model should be interpreted cautiously for clinical cases of SSc. Further and more comprehensive studies of the effects of geniposide for SSc treatment should be performed.

In conclusion, BLM treatment resulted in up-regulation of the expression of biomarkers in mesenchymal cells and down-regulation of the biomarkers in ECs. Tube formation ability in HUVECs was also down-regulated after BLM treatment. These effects were suppressed by the addition of a geniposide treatment. The key factors in the EndMT and mTOR signaling pathways were also down-regulated by geniposide treatment. Therefore, geniposide might be a potential therapeutic candidate for treatment of the vasculopathy that occurs in SSc patients.

Acknowledgements

The authors would like to thank the National Natural Science Foundation of China (to Qing Qi, 81573976), the Natural Science Foundation of Guangdong Province (to Qing Qi, 2015A030313341), the Science and Technology Planning Project of Guangdong Province (to Qing Qi, 2014A020221029), the 2012 Excellent Young Scientist Foundation from Guangzhou University of Chinese Medicine (to Qing Qi, 20120102), and the China Scholarship Council (to Qing Qi, 201408440370) for financial support. The US National Institutes of Health (to Xiao-Dong Zhou, NIAID 1U01AI09-090-01) also funded this project.

Disclosure of conflict of interest

None.

Authors' contribution

Yueping Mao, Yongzhen Tian, and Ke Zhu performed the *in vivo* and *in vitro* studies, analyzed the data, and wrote the manuscript. Xushan Cha and Minghua Wu contributed critical discussion of the manuscript. Xiaodong Zhou and Qing Qi contributed to the discussion and design of an earlier version of the manuscript. All authors read and approved the final manuscript version.

Address correspondence to: Dr. Qing Qi, Department of Dermatology, The First Affiliated Hospital, Guangzhou University of Chinese Medicine, Jichang Road 16, Guangzhou 510405, China. Tel: +862036591826; E-mail: qing_qi@hotmail.com; Dr. Xiaodong Zhou, Division of Rheumatology and Clinical Immunogenetics, Department of Internal Medicine, University of Texas Health Science Center at Houston, 6431 Fannin, Houston 77030, Texas, USA. Tel: +17139227119; E-mail: Xiaodong.Zhou@uth.tmc.edu

References

[1] Trojanowska M. Cellular and molecular aspects of vascular dysfunction in systemic sclerosis. Nat Rev Rheumatol 2010; 6: 453-460.

[2] Pattanaik D, Brown M, Postlethwaite AE. Vascular involvement in systemic sclerosis (scleroderma). J Inflamm Res 2011; 4: 105-125.

[3] Piera-Velazquez S, Li Z, Jimenez SA. Role of endothelial-mesenchymal transition (EndoMT) in the pathogenesis of fibrotic disorders. Am J Pathol 2011; 179: 1074-1080.

[4] Frid MG, Kale VA, Stenmark KR. Mature vascular endothelium can give rise to smooth muscle cells via endothelial-mesenchymal transdifferentiation: in vitro analysis. Circ Res 2002; 90: 1189-1196.

[5] Zeisberg EM, Tarnavski O, Zeisberg M, Dorfman AL, Mcmullen JR, Gustafsson E, Chandraker A, Yuan X, Pu WT, Roberts AB, Neilson EG, Sayegh MH, Izumo S, Kalluri R. Endothelial-to-mesenchymal transition contributes to cardiac fibrosis. Nat Med 2007; 13: 952-961.
[6] Arciniegas E, Frid MG, Douglas IS, Stenmark KR. Perspectives on endothelial-to-mesenchymal transition: potential contribution to vascular remodeling in chronic pulmonary hypertension. Am J Physiol Lung Cell Mol Physiol 2007; 293: L1-8.
[7] Li J, Bertram JF. Review: endothelial-myofibroblast transition, a new player in diabetic renal fibrosis. Nephrology (Carlton) 2010; 15: 507-512.
[8] Kizu A, Medici D, Kalluri R. Endothelial-mesenchymal transition as a novel mechanism for generating myofibroblasts during diabetic nephropathy. Am J Pathol 2009; 175: 1371-1373.
[9] Potts JD, Runyan RB. Epithelial-mesenchymal cell transformation in the embryonic heart can be mediated, in part, by transforming growth factor β. Dev Biol 1989; 134: 392-401.
[10] Yamamoto T. The bleomycin-induced scleroderma model: what have we learned for scleroderma pathogenesis? Arch Dermatol Res 2006; 297: 333-344.
[11] Yamamoto T, Takagawa S, Katayama I, Yamazaki K, Hamazaki Y, Shinkai H, Nishioka K. Animal model of sclerotic skin. I: local injections of bleomycin induce sclerotic skin mimicking scleroderma. J Invest Dermatol 1999; 112: 456-462.
[12] Ishikawa H, Takeda K, Okamoto A, Matsuo S, Isobe K. Induction of autoimmunity in a bleomycin-induced murine model of experimental systemic sclerosis: an important role for CD4+ T cells. J Invest Dermatol 2009; 129: 1688-1695.
[13] Batteux F, Kavian N, Servettaz A. New insights on chemically induced animal models of systemic sclerosis. Curr Opin Rheumatol 2011; 23: 511-518.
[14] Hashimoto N, Phan SH, Imaizumi K, Matsuo M, Nakashima H, Kawabe T, Shimokata K, Hasegawa Y. Endothelial-mesenchymal transition in bleomycin-induced pulmonary fibrosis. Am J Respir Cell Mol Biol 2010; 43: 161-172.
[15] Taniguchi T, Asano Y, Akamata K, Noda S, Takahashi T, Ichimura Y, Toyama T, Trojanowska M, Sato S. Fibrosis, Vascular Activation, and Immune Abnormalities resembling systemic sclerosis in bleomycin-treated Fli-1-haploinsufficient mice. Arthritis Rheumatol 2014; 67: 517-526.
[16] Toyama T, Asano Y, Akamata K, Noda S, Taniguchi T, Takahashi T, Ichimura Y, Shudo K, Sato S, Kadono T. Tamibarotene ameliorates bleomycin-induced dermal fibrosis by modulating phenotypes of fibroblasts, endothelial cells, and immune cells. J Invest Dermatol 2016; 136: 387-398.
[17] Markwald RR, Fitzharris TP, Smith WN. Structural analysis of endocardial cytodifferentiation. Dev Biol 1975; 42: 160-180.
[18] Potenta S, Zeisberg E, Kalluri R. The role of endothelial-to-mesenchymal transition in cancer progression. Br J Cancer 2008; 99: 1375-1379.
[19] Liebner S, Cattelino A, Gallini R, Rudini N, Iurlaro M, Piccolo S, Dejana E. Beta-catenin is required for endothelial-mesenchymal transformation during heart cushion development in the mouse. J Cell Biol 2004; 166: 359-367.
[20] Nawshad A, Medici D, Liu CC, Hay ED. TGFbeta3 inhibits E-cadherin gene expression in palate medial-edge epithelial cells through a Smad2-Smad4-LEF1 transcription complex. J Cell Sci 2007; 120: 1646-1653.
[21] Kokudo T, Suzuki Y, Yoshimatsu Y, Yamazaki T, Watabe T, Miyazono K. Snail is required for TGFbeta-induced endothelial-mesenchymal transition of embryonic stem cell-derived endothelial cells. J Cell Sci 2008; 121: 3317-3324.
[22] Medici D, Hay ED, Olsen BR. Snail and slug promote epithelial-mesenchymal transition through β-catenin-T-cell factor-4-dependent expression of transforming growth factor-β3. Mol Biol Cell 2008; 19: 4875-4887.
[23] Laplante M, Sabatini D. mTOR signaling in growth control and disease. Cell 2012; 149: 274-293.
[24] Wei Z, Gang C, Ren JG, Zhao YF. Bleomycin induces endothelial mesenchymal transition through activation of mTOR pathway: a possible mechanism contributing to the sclerotherapy of venous malformations. Br J Pharmacol 2013; 170: 1210-1220.
[25] Qi Q, Mao Y, Yi J, Li D, Zhu K, Cha X. Anti-fibrotic effects of astragaloside iv in systemic sclerosis. Cell Physiol Biochem 2014; 34: 2105-2116.
[26] Liu J, Fei Y, Zheng X, Jing J, Hu Y. Geniposide, a novel agonist for GLP-1 receptor, prevents PC12 cells from oxidative damage via MAP kinase pathway. Neurochem Int 2007; 51: 361-369.
[27] Peng CH, Huang CN, Hsu SP, Wang CJ. Pentaacetyl geniposide-induced apoptosis involving transcription of NGF/p75 via MAPK-mediated AP-1 activation in C6 glioma cells. Toxicology 2007; 238: 130-139.
[28] Liaw J, Chao YC. Effect of in vitro and in vivo aerosolized treatment with geniposide on tracheal permeability in ovalbumin-induced guinea pigs. Eur J Pharmacol 2002; 433: 115-121.

[29] Wu SY, Wang GF, Liu ZQ, Rao JJ, Lü L, Xu W, Wu SG, Zhang JJ. Effect of geniposide, a hypoglycemic glucoside, on hepatic regulating enzymes in diabetic mice induced by a high-fat diet and streptozotocin. Acta Pharmacol Sin 2009; 30: 202-208.
[30] Lee P, Lee J, Choi SY, Lee SE, Lee S, Son D. Geniposide from Gardenia jasminoides attenuates neuronal cell death in oxygen and glucose deprivation-exposed rat hippocampal slice culture. Biol Pharm Bull 2006; 29: 174-176.
[31] Yin F, Liu J, Zheng X, Guo L, Xiao H. Geniposide induces the expression of heme oxygenase-1 via PI3K/Nrf2-signaling to enhance the antioxidant capacity in primary hippocampal neurons. Biol Pharm Bull 2010; 33: 1841-1846.
[32] Park JH, Yoon J, Lee KY, Park B. Effects of geniposide on hepatocytes undergoing epithelial-mesenchymal transition in hepatic fibrosis by targeting TGFβ/Smad and ERK-MAPK signaling pathways. Biochimie 2015; 113: 26-34.
[33] Medici D, Potenta S, Kalluri R. Transforming growth factor-β2 promotes Snail-mediated endothelial-mesenchymal transition through convergence of Smad-dependent and Smad-independent signalling. Biochem J 2011; 437: 515-520.
[34] Welch-Reardon KM, Wu N, Hughes CC. A role for partial endothelial-mesenchymal transitions in angiogenesis? Arterioscler Thromb Vasc Biol 2015; 35: 303-308.
[35] Grande MT, López-novoa JM. Fibroblast activation and myofibroblast generation in obstructive nephropathy. Nat Rev Nephrol 2009; 5: 319-328.
[36] Tang R, Li Q, Lv L, Dai H, Min Z, Ma K, Liu B. Angiotensin II mediates the high-glucose-induced endothelial-to-mesenchymal transition in human aortic endothelial cells. Cardiovasc Diabetol 2010; 9: 31.
[37] Stawski L, Han R, Bujor AM, Trojanowska M. Angiotensin II induces skin fibrosis: a novel mouse model of dermal fibrosis. Arthritis Res Ther 2012; 14: R194.
[38] Mendoza FA, Sonsoles PV, Farber JL, Carol FB, Jimenez SA. Endothelial cells expressing endothelial and mesenchymal cell gene products in Systemic Sclerosis-associated interstitial lung disease lung tissues. Arthritis Rheum 2015; 68: 210-217.
[39] Nicolosi PA, Tombetti E, Maugeri N, Roverequerini P, Brunelli S, Manfredi AA. Vascular remodelling and mesenchymal transition in systemic sclerosis. Stem Cells Int 2016; 2016: 4636859.
[40] Matucci-Cerinic M, Kahaleh B, Wigley FM. Review: evidence that systemic sclerosis is a vascular disease. Arthritis Rheum 2013; 65: 1953-1962.
[41] Barrallo-Gimeno A, Nieto MA. The Snail genes as inducers of cell movement and survival: implications in development and cancer. Development 2005; 132: 128-130.
[42] Cooley BC, Nevado J, Mellad J, Yang D, St Hilaire C, Negro A, Fang F, Chen G, San H, Walts AD, Schwartzbeck RL, Taylor B, Lanzer JD, Wragg A, Elagha A, Beltran LE, Berry C, Feil R, Virmani R, Ladich E, Kovacic JC, Boehm M. TGF-β signaling mediates endothelial-to-mesenchymal transition (EndMT) during vein graft remodeling. Sci Transl Med 2014; 6: 227ra234.